New insights on the evolution of the Linosa volcano (Sicily Channel) from the study of its submarine portions

New insights on the evolution of the Linosa volcano (Sicily Channel) from the study of its submarine portions

C. Romagnoli[a,*], V. Belvisi[a], S. Innangi[b], G. Di Martino[b], R. Tonielli[b]

[a] Dipartimento di Scienze Biologiche, Geologiche ed Ambientali, Università di Bologna, Piazza di Porta S. Donato 1, 40127 Bologna, Italy
[b] ISMAR-CNR, Calata Porta di Massa, 80, 80133 Napoli, Italy

ARTICLE INFO

Editor: Michele Rebesco

Keywords:
Submarine volcanoes
Multibeam bathymetry
Morphometry
Eruptive cones

ABSTRACT

Linosa Island represents the emergent tip of a mostly submarine, much wider volcanic edifice, with at least 96% of its areal extent lying below sea level. Marine geological surveys carried out in 2016 and 2017 allowed to reconstruct the submarine portions of Linosa and to characterize the main volcanic features, providing new, unexpected insights on the evolution of this little-explored volcanic complex. In particular, the submarine setting of the NW offshore is represented by a ~10-km long volcanic belt punctuated by a number of small eruptive cones, appearing more recent with respect to the assumed Mid/Late-Quaternary age of volcanism on the island. This evidence suggests that the growth of the volcanic edifice has likely been more complex than that claimed on the base of subaerial volcanism only, and supports a north-westward migration of the activity over time. The submarine southern flank of the volcanic edifice is also characterized by eccentric eruptive cones, but mostly without evidences of recent activity. The main processes responsible for the growth and evolution of Linosa volcano and their possible relative chronology are discussed in the framework of what previously known on the base of the limited subaerial portions, with implications on the potential hazard of the volcanic edifice (considered as not-active in recent times). Similarity with the Pantelleria volcano, located in the NW Sicily Channel, are also evidenced, especially for what regards the distribution and morphometric characteristics of eruptive cones occurring in the submarine portions of both islands.

1. Introduction

Linosa is a small volcanic island (about 6 km^2) in the Sicily Channel (Central Mediterranean Sea, Fig. 1). Its morphology (culminating at 196 m a.s.l.) is the result of volcanic subaerial activity that led it to emerge in the Quaternary (Lanzafame et al., 1994). Up to know the very scarce knowledge on its submarine extension led to consider this volcanic edifice as extinct. The recent acquisition of multibeam bathymetry down to the base of the volcanic complex indicated a much wider submarine extension than expected, down to a depth of 1000 m (Tonielli et al., 2019). Overall the volcanic edifice extends and for about 20 km in the NW SE direction, along which the main structural system of the Sicily Channel is oriented, as already suggested for the limited subaerial portions (Lanti et al., 1988; Rossi et al. 1990 and 1996).

This paper focuses on the main volcanic features observed in the wide submarine portions of Linosa (accounting for about 96% of the whole edifice extension) through high resolution multibeam bathy metry, integrated by some high resolution (Sparker) seismic profiles. The reconstructed setting and the morphology of the submarine flanks, punctuated by a number of individual eruptive cones, provide new insights in the development and evolution of the volcanic edifice, enhancing a regional tectonic control on its development and suggesting to post date its last eruptive activity. Furthermore, the reconstructed setting for Linosa is very similar to that of the Pantelleria volcano in the northwestern Sicily Channel (Fig. 1). The morphometric analysis of the submarine cones mapped at Linosa is thus discussed also through comparison with similar features previously studied on the northern submarine flank of Pantelleria (Calarco, 2011; Bosman et al., 2011), where the last eruption occurred in 1891 offshore the NW coast of the island (Riccò, 1892; Conte et al., 2014), and in other volcanic settings where recent submarine activity occurred.

2. Geological setting

Linosa belongs to the Pelagian Archipelago (together with Lampedusa and Lampione, being not volcanic in origin) located in the central southern Sicily Channel, about 160 km off the Tunisian coast and 180 km off the west of Sicily (Fig. 1). The Sicily Channel is a

* Corresponding author.
E-mail address: claudia.romagnoli@unibo.it (C. Romagnoli).

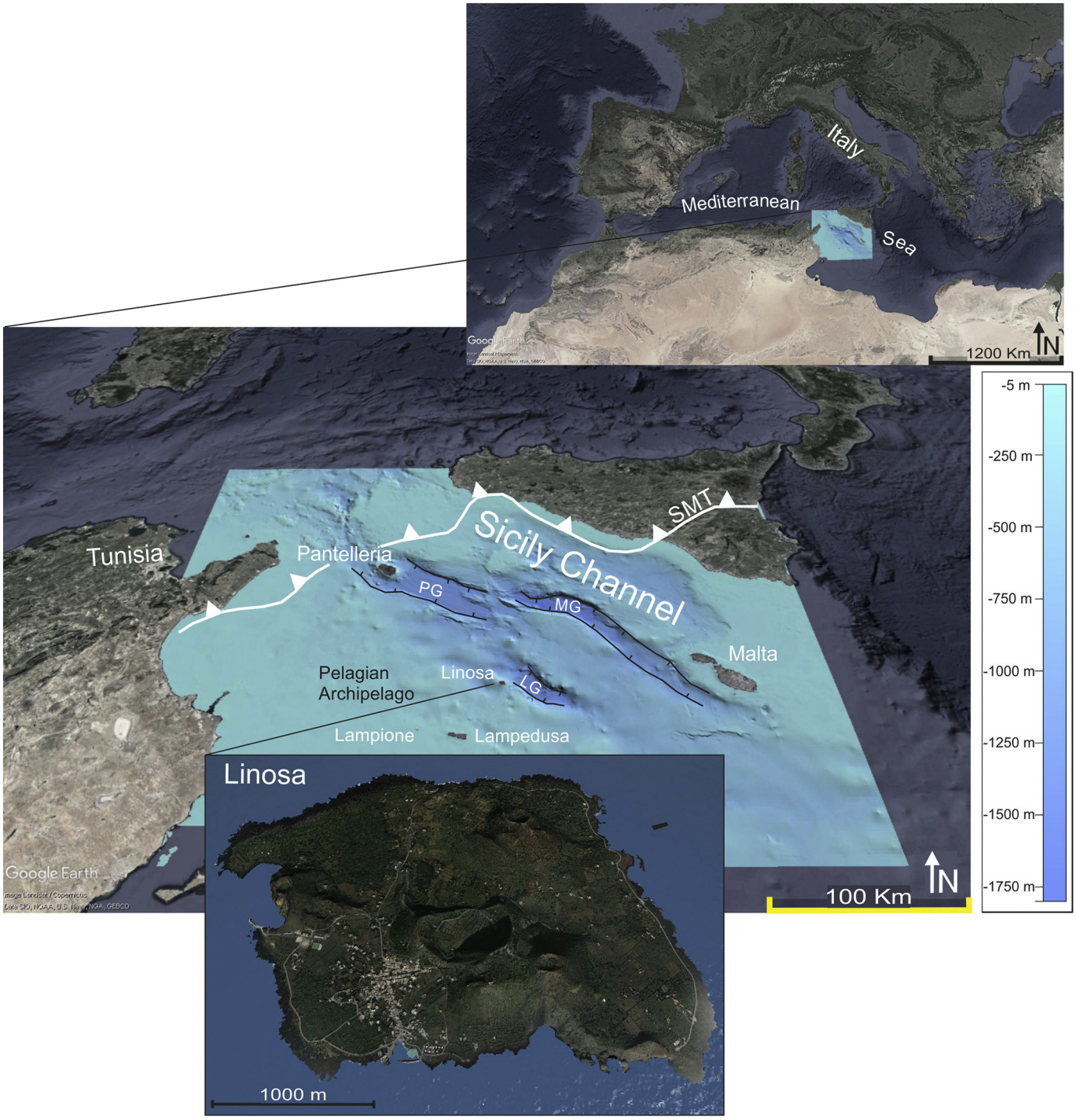

Fig. 1. Location map of Linosa Island in the Sicily Channel. PG: Pantelleria graben, MG: Malta graben, LG: Linosa graben. SMT: Sicilian-Maghrebian Thrust.

complex rift zone within the continental African plate in the foreland of the Sicilian Maghrebian Chain (a thrust and fold belt) and is characterized by three deep tectonic troughs, namely the Pantelleria, Linosa, and Malta grabens (Civile et al., 2010; Fig. 1). These features are referred to Neogene Quaternary crustal stretching processes principally controlled by NW SE directed sub vertical normal faults, that favored intense magma rising. Anorogenic volcanism in the Sicily Channel was active from Plio Pleistocene onward (with mostly alkaline to peralka line affinity; Calanchi et al., 1989). According to some Authors (Civile et al., 2010, and references herein), the Sicily Channel is an example of intraplate "passive" rift, where volcanism is a consequence of tensional stresses on the lithosphere due to the regional stress field. However, the reconstruction of tectonic mechanisms responsible for the development of the rifting zone is still uncertain, and the relationships among the deep crustal structure, the tectonic and volcano tectonic processes and the evolution of volcanism are still to be better defined (Civile et al., 2010).

The island of Linosa is the top of a composite volcano that extends at the southwestern shoulder of homonym through (having max. depth of 1580 m; Colantoni, 1975). Its growth is the result of a volcanic history dated from ~1.06 Ma to 0.5 Ma which has been divided into three main eruptive stages, separated by two major gaps corresponding to palaeosoils (Grasso et al., 1991; Lanzafame et al., 1994; Rossi et al., 1996). During these stages, hydromagmatic and magmatic eruptions produced

tuff rings, tuff cones, scoria and spatter cones and extended lava flows (Rossi et al., 1996). Volcanic rocks at Linosa show a limited compositional range, from alkali basalts to hawaiites/mugearites, with rare, more evolved compositions in pyroclastic products (Rossi et al., 1996). According to paleomorphological reconstructions and the analysis of the provenance of pyroclastic deposits outcropping at Linosa, some of the eruptive centres active during the early growth of the island were located offshore and were then almost completely eroded by the sea (Lanti et al., 1988; Lanzafame et al., 1994; Rossi et al., 1996). The shallow water portions of the volcanic edifice (at depth < −100/ 150 m) are, in fact, largely dismantled, as also witnessed by the oc currence of wide insular shelves on the submarine SE and NW flanks of the island (Romagnoli, 2004). However, no data are available yet for the age of the wide submarine portions of Linosa.

3. Data and methods

The submarine area of Linosa Island was investigated during two oceanographic cruises organized by IAMC (now ISMAR, Institute for Marine Sciences) of the National Research Council (CNR) of Naples (Italy), carried out in August 2016 and September 2017 aboard the R/V *Minerva Uno*. High resolution bathymetry was acquired from −15 m to about −1000 m around the island by employing a multibeam echosounder with a frequency of 455 kHz (Teledyne Reson SeaBat 7125) in shallow water and a frequency of 50 kHz (Teledyne Reson SeaBat 7160) at greater depth (see Innangi et al., 2018 and Tonielli et al., 2019, for details). Positioning was obtained through Differential Global Positioning System (DGPS). Data were processed using the software Teledyne PSD 4.1 and were merged and gridded in a 10 m cell size for the production of the final DEM in the UTM projection, Zone 33, WGS84, being the base for morphological analysis and mapping of seabed (Fig. 2). This has been integrated with multibeam data previously acquired in the shallow water area (2 10 m depth, grid 1 × 1 m) with Reson SeaBat 8125 for the Marine Protected Area (Coastal Consulting Exploration, 2008).

High resolution (Chirp and Sparker Geo Source 1000) seismic profiles were collected on s elected areas to characterize the nature of the

Table 1
Description of main parameters used in the morphometric analyses and their measurement.

Parameter	Unit	Description
Typology	–	Shape of cone in section and in map
Zs	m	Summit depth of volcanic cone
Zb	m	Basal depth of volcanic cone
dmax (S)[a]	m	Maximum cone summit diameter
dmax (B)	m	Maximum cone basal diameter
dmin (S)[a]	m	Minimal cone summit diameter
dmin (B)	m	Minimal cone basal diameter
bsr	–	Cone basal ratio, defined as dmax(B)/dmin(B)
Wbc	m	Cone width ratio, calculated by (dmax(B) + dmin(B)) / 2
hmax	m	Maximum difference between the depths of the top and the base of the volcanic cone
AR	–	Cone aspect ratio, calculated by hmax/Wbc
Ac	km^2	Cone basal area
Vc	km^3	Volume of cone
Smax	Degree (°)	Maximum slope angle

[a] The summit diameter is given only for flat-topped cones.

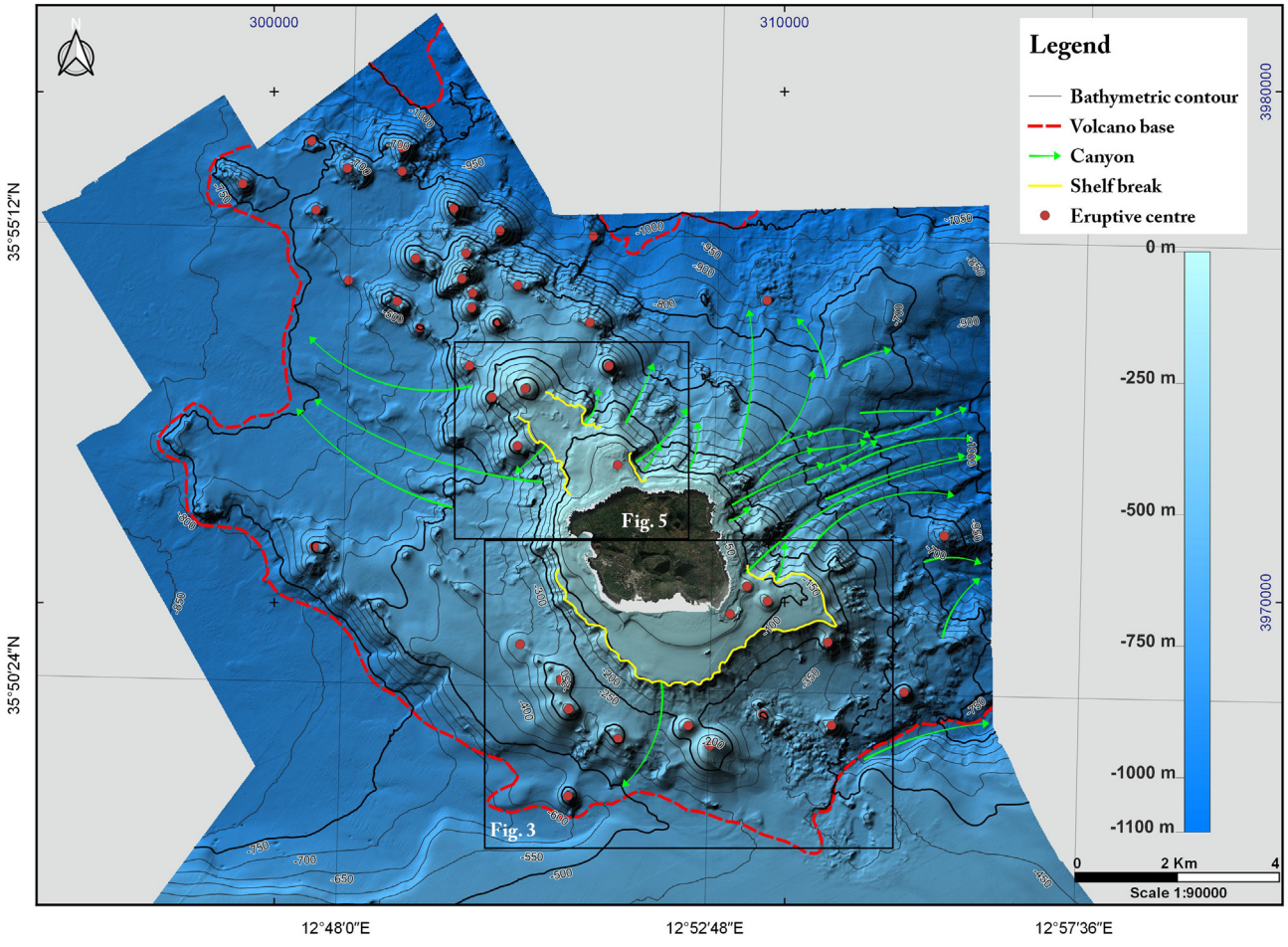

Fig. 2. Bathymetric map of Linosa with main morphological lineaments. The location of following figures is indicated in the boxes.

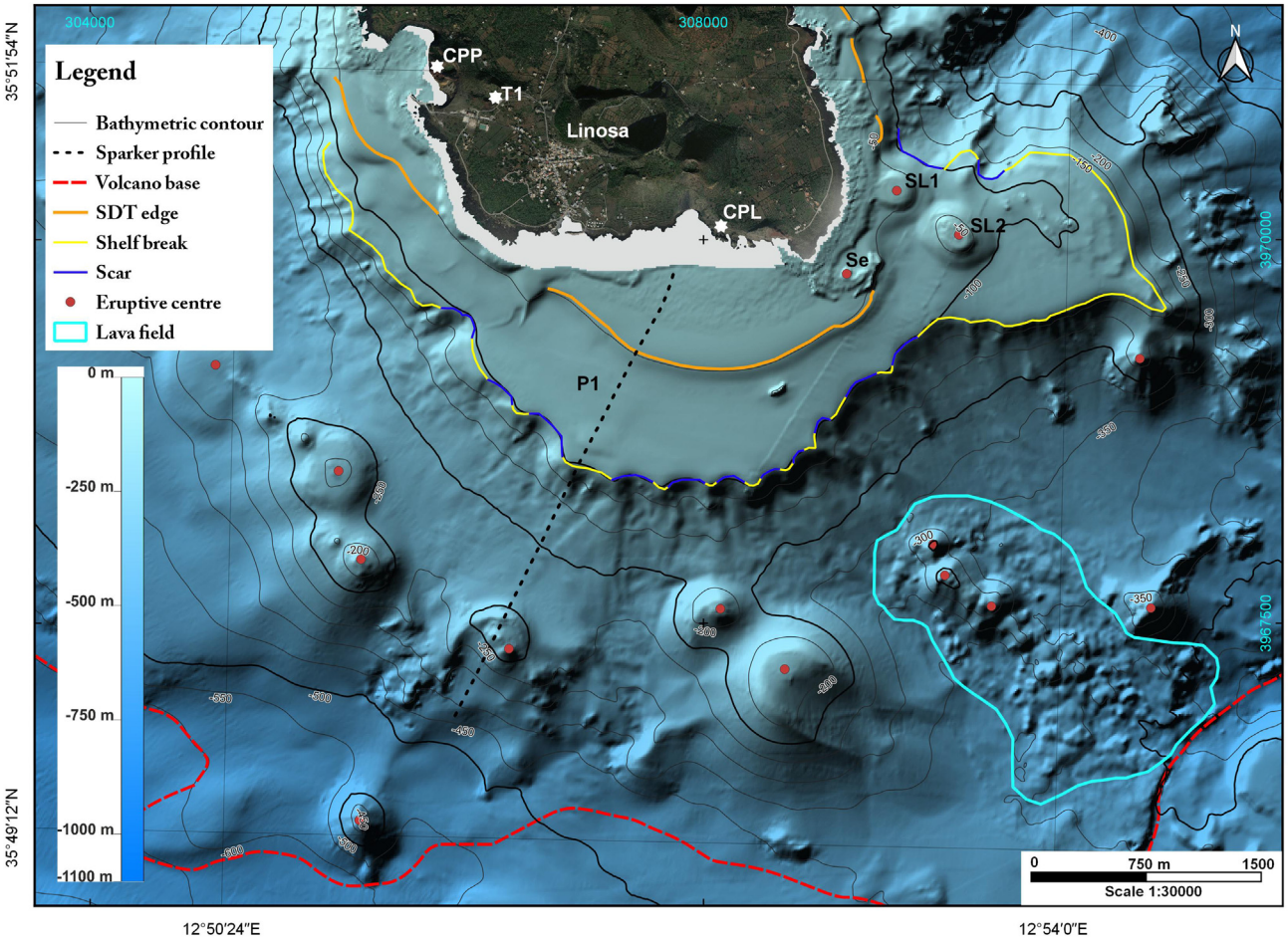

Fig. 3. Shaded-relief image of the southern portion of Linosa with indication of morphological lineaments described in the text. Submarine eruptive centres of Secca di Levante (SL1 and SL2) and Secchetella (Se) are indicated. Location of eruptive vents inland (from Lanzafame et al., 1994) is indicated by stars (CPP: Cala Pozzolana di Ponente; T1: Timpone 1; CPL: Cala Pozzolana di Levante). Location of seismic line of Fig. 4 is also indicated.

seabed. They were processed with Geosuite Allworks and some representative lines are given in Section 4. The main morphologic and volcanologic features recognized in the submarine flanks of Linosa have been mapped from the coast to its submarine base (Fig. 2).

3.1. Morphometric analysis

A specific morphometric investigation of the volcanic cones mapped on the Linosa submarine flanks was carried out, focusing on structures at least 40 m high from the seafloor. The morphological and morphometric parameters considered for the analysis (Table 1) are the same used for the characterization of scoria cones in other geological context, both in subaerial and subaqueous environments (Romero Ruiz et al., 2000; Doniz Páez et al., 2008; Favalli et al., 2009; Mitchell et al., 2012; Fornaciai et al., 2012; Kerezsturi et al., 2013; Spatola et al., 2018). These parameters are extracted from the high resolution DEM (10 × 10 m, 1 × 1 m in shallow water) by using specific tools of the *Global Mapper* software, that has been also used for 3D representations (see figures in ESM).

On the base of their shape on plant and section view, the observed submarine cones were attributed to five different typologies (conical/subconical, elliptical/subelliptical, composite, flat topped and star-shaped). The basal ratio (bsr) value or "cone elongation" (Doniz Páez, 2015) has been considered in order to discriminate circular vs. elliptical shape ($\leq$ or $\geq$1.3 respectively, see Table 1ESM). Composite ones are the result of the coalescence of simple conical shapes. The approach of Favalli et al. (2009)has been applied for estimating the hmax as the maximum elevation above a fitting basal plane of the volcanic cone, in the case of cones rising from a considerable dipping plane, for which the difference between depth of the top and base might be different along the opposite sides of the cone. The aspect ratio (AR), i.e. the ratio between hmax and the cone width ratio (Wbc), is another used parameter, frequently adopted for classification (Favalli et al., 2009; Mitchell et al., 2012; Fornaciai et al., 2012); it can differ for cones having the same area. Area (Ac), volume (Vc) and maximum slope (Smax) have been also calculated through *Global Mapper* tools (Table 1ESM). Since craters are not or rarely observed at the scale of the submarine DTM in the analyzed scoria cones, related morphological parameters are not considered.

4. Results

4.1. Bathy morphological setting of Linosa

The bathymetric map of Linosa shows the extension of the volcanic edifice, with a width in the order of 5 km from the coast in the southern flank, becoming larger on other submarine flanks. In particular, it is clearly elongated in the NW SE direction for over 10 km from the island coast (Fig. 2). The base of the volcanic edifice is located at about 1000 m depth in the northwestern and northeastern sectors; it shallows to −750 m depth towards the west and southeast, and to −450 m in the southern flank. A NW SE oriented (N132°SE) escarpment, 200 m high and being likely of tectonic origin delimits the submarine western flank between 500 and 750 m depth on a length of about 6 7 km

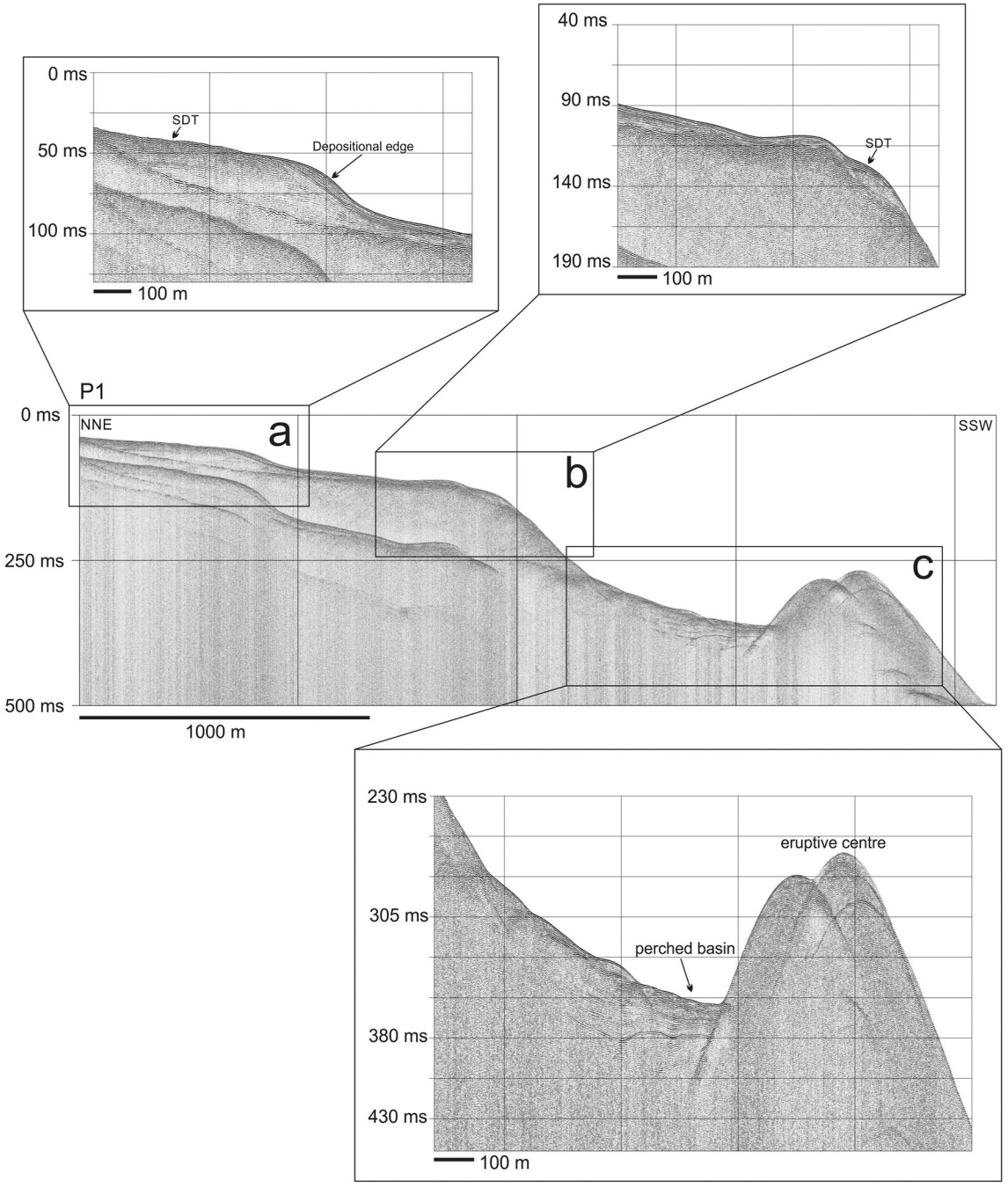

Fig. 4. Sparker profile (location in Fig. 3) on the southern flank of Linosa, and zooms showing the prograding terraced wedge (Submerged Depositional Terrace, SDT) in the inner shelf (a) and at the shelf edge (b). In (c) the profile shows a submarine eruptive centre rising from the submarine southern flank of Linosa and damming a small perched basin.

(Fig. 2), corresponding to a marked increase in the slope gradient (20 36°).

From the coast, insular shelves are widely present to the NW and all around the S sector of the island, carving the shallow water portions of the volcanic edifice (Fig. 2). These features are characterized by gently sloping (commonly 2 5°steep) surfaces extending from the coastline to the shelf break, while a sharp increase in gradient occurs passing to the submarine slopes of the island (up to 30 33°). Where shelves are reduced or lacking, i.e. in the northeastern, eastern and part of the wes tern sectors, the submarine flank is steeper and erosional features (such as canyons) carve the submarine flanks from shallow water down to the their base, alternating with volcanic ridges in radial or slightly diverging networks (Fig. 2). These canyons are the seat of active remobilization, as suggested by the occurrence of widespread sediment waves on their floor. These are very common features on the submarine flanks of volcanic islands (Pope et al., 2018) where canyons are responsible for the transfer of volcaniclastic sediments at higher depth through gravity driven currents (Babonneau et al., 2013).

4.1.1. Submarine volcanic structures

Several volcanic structures are recognized in the seafloor around Linosa. They are observed either in the nearshore, as the submerged prolongation of subaerial lava flows that entered the sea, or as isolated features on the submarine flanks, unrelated to the subaerial morphology. The progradation of lava flows on the insular shelf is observed around great part of Linosa Island, being characterized by distinctive

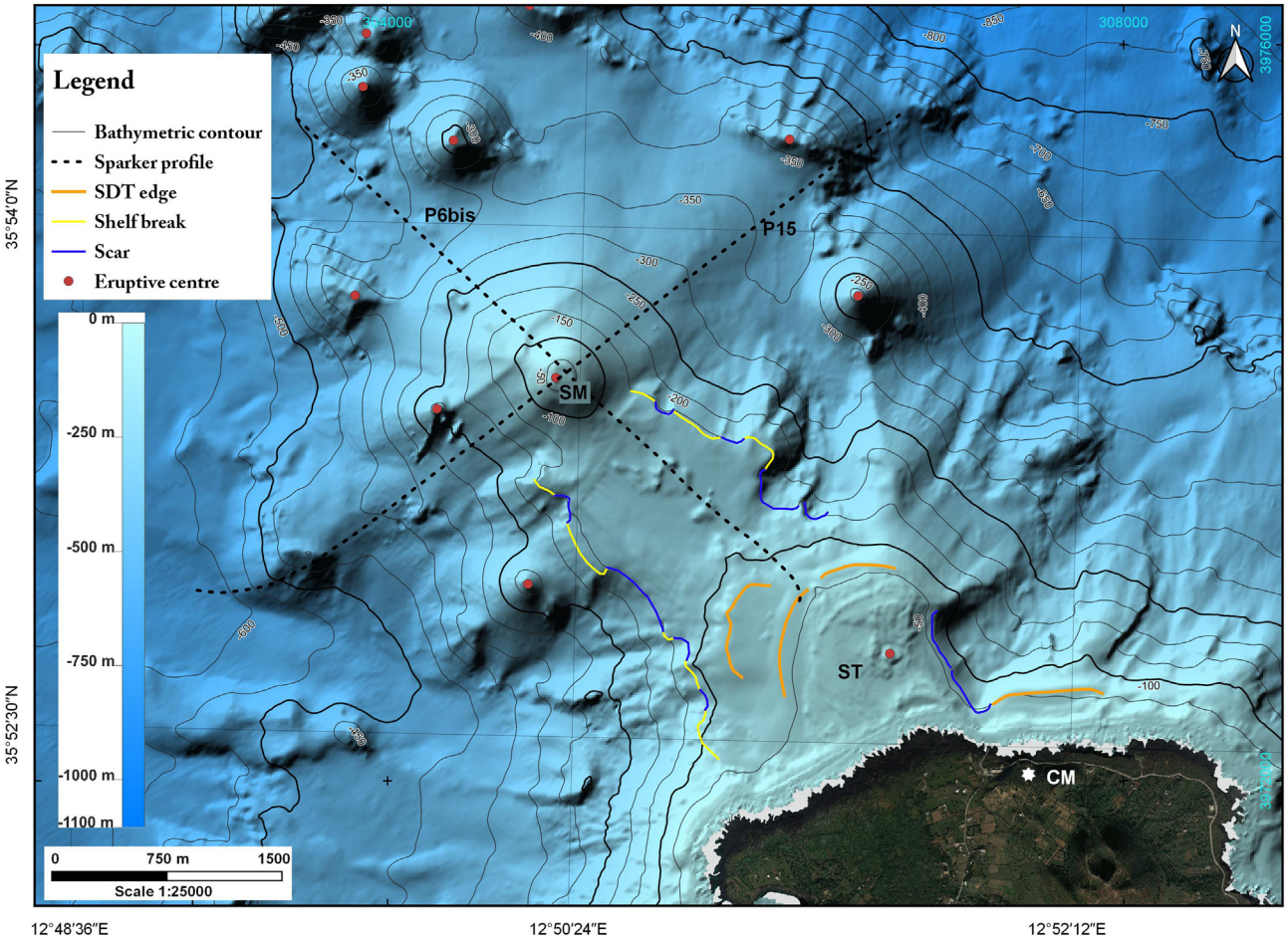

Fig. 5. Shaded-relief image of the north-western portion of Linosa with indication of morphological lineaments described in the text. Submarine eruptive centres of Secca di Tramontana (ST) and Secca Maestra (SM) are indicated. Location of Cala Mannarazza eruptive vent inland (CM, from Lanzafame et al., 1994) is indicated by a star. Location of seismic lines of Fig. 6 is also indicated.

lobate shape, low relief and rugged or smooth surface texture (Figs. 1ESM and 2ESM). Their relationships with the subaerial eruptive centres are not addressed in this paper. Deep water submarine lava fields have been also observed in the submarine flanks of Linosa at various depth, such as to the southeast of the island (Figs. 3 and 1ESM). Here a rough and irregular terrain is observed at depth of about 300 500 m around three small scale eruptive centres and elongates downslope, for a total area of about 5.86 km^2. Its bathymetric relief and seismic appearance is similar to that of other volcanic outcrops ob served at Vulcano (Romagnoli et al., 2013) and Stromboli (Di Roberto et al., 2008; Bosman et al., 2009) volcanic islands, where they have been interpreted as pillow lava fields, so it could be considered the product of a submarine eruption, not yet buried by marine sedi mentation. This is also supported by its localized distribution around, and at the foot, of three small eruptive centres (Figs. 3 and 1ESM) that most likely represent the source area. As an alternative hypothesis, the hummocky morphology might be the result of a slope failure affecting the southern submarine flank of Linosa and related to slide scars car ving the shelf edge (Fig. 3), producing a blocky field of debris or a debris avalanche deposit (similarly to what observed in other volcanic contexts; Watts and Masson, 1995; Romagnoli et al., 2009a and 2009b), although these deposits commonly show a more widespread extension and larger scales. Further investigations (such as the acquisition of extremely high resolution bathymetric data through AUV or ROV images, see for instance Clague et al., 2019 and Somoza et al., 2017) and samplings could allow to better characterize the nature and source area of submarine lava flows/volcaniclastic deposits at Linosa.

The northwestern and southern flanks of Linosa appear punctuated by a large number of eruptive centres that have been mapped (Fig. 2) and characterized from a morphologic point of view. They occur both in shallow and in deep water, the former ones being mostly represented by remnants of eruptive vents lying on insular shelves (i.e. above −100/130 m depth). Apart from the deeply eroded and scarcely preserved ones, all eruptive centres lying on the submarine flanks of Linosa are the subject of specific morphometric analyses (Section 4.2).

4.1.2. Insular shelves and shallow water eruptive centres

A well developed insular shelf with semi circular geometry is present in shallow water around the southern portion of Linosa, where it extends from the coast to its outer edge for about 0.6 1.7 km in width, for a total area of ~5800 m^2 (Figs. 3 and 1ESM). The shelf edge depth is mostly in the range −100/−130 m, but small scale landslide scars affect the insular shelf all along its southern edge, possibly reducing its original extension and depth (Fig. 3). On the inner shelf, a main slope break at around −45/−50 m with curvilinear shape (in orange in Fig. 3) extends with good lateral continuity along the southern and southwestern shelf. From seismic profiles it appears to correspond to the depositional edge (*offlap break* or *rollover depth*) of a sedimentary body with wedge shaped geometry and internal prograding structure lying on the shelf erosive surface (Submerged Depositional Terraces, SDT, in Figs. 3 and 4a). A deeper prograding body is also locally ob served at the shelf edge, having a depositional edge at about 95 105 m (Fig. 4b; not mapped in Fig. 3 due to its limited extension). Similar submarine prograding wedges are commonly observed on the steep and

high energy shelves of insular volcanoes, where they are considered to form through the subaqueous reworking of volcaniclastic deposits due to seaward transport from the surf zone and shoreface during storms (Chiocci and Romagnoli, 2004; Quartau et al., 2010, 2014, 2015; Mitchell et al., 2012; Casalbore et al. 2017 and 2018 and references herein). The occurrence at Linosa of a set of SDTs lying at different depths made of volcaniclastic sediments, was previously observed by Romagnoli (2004) and related to the reworking and deposition of se diments on the shelf during stillstands of the relative sea level at a depth lower than the present one.

On the shelf, the eroded remnants of small eccentric vents are recognized offshore the southeastern edge of the island (Fig. 3). Here two sub circular truncated cones with diameter around 360/450 m (*Secca di Levante*, SL1 and SL2 in Figs. 3, 1ESM and 2ESM) rise to a depth of 30/ 33 m from the shelf surface with flattened summits, characterized by irregular surface. More to the south, very close to the island, a further half rounded feature around 490 m in diameter (*Secchetella*, Se in Figs. 3, 1ESM and 2ESM) is present with top at depth of 15 17 m. It is characterized by concentric relief, due to possible erosion remnants of a highly dismantled eruptive cone.

A well developed, NNW SSE elongated insular shelf with a trans versal width of about 350 750 m is also observed offshore the north western sector of the island (Figs. 2 and 5). The shelf break depth is in the range −100/−150 m, being locally indented by slide scars (Fig. 5). Some morphological irregularities are present on the shelf surface, re presenting the remnants of deeply eroded volcanic structures and vents. A sub-rounded feature, characterized by concentric relief at its summit, is observed close to the northern coast of Linosa in correspondence of *Secca di Tramontana* (ST in Figs. 5 and 3ESM; min. depth 15 m), likely representing the erosion remnant of a dismantled eruptive cone. It is affected by a main slope break at about 110 m corresponding to the shelf break, and is deeply eroded on its eastern side. Overall, the northwestern shelf appears as sediment starved, apart from the occur rence of small scale terraced deposits (SDTs) creating some bathymetric steps with curvilinear development at depths of 55 75 m around *Secca di Tramontana* (orange lines in Fig. 5) and in front of the central northern coast of Linosa. To the NW, about 2 km far from the island, the shelf connects with an eruptive cone (*Secca Maestra*, SM in Figs. 5 and 3ESM) showing a very regular conical shape with top at −38 m, not affected by erosion characterizing the other volcanic features on the shelf. On seismic profiles (Fig. 6) it appears, in fact, as a very regular cone, and the deposits at its foot overlap the shelf erosive surface (Fig. 6a).

4.1.3. Eruptive centres on the deeper submarine flanks of Linosa

Below the insular shelves, a number of eruptive centres are recognized on the submarine flanks of Linosa, rising from various depth ranges (down to a maximum depth around −900 m; Fig. 2). These small monogenetic volcanoes are interpreted as cinder/scoria cones because of their size and morphologic characteristics (Sigurdsson et al., 2000; Doniz Páez, 2015 and references herein). In the northwestern offshore of the island, over 20 eruptive centres are aligned to form a NW SE oriented, up to 8 10 km long belt, made of single or coalescing monogenetic volcanoes, for a total area of 8.10 km^2 (Figs. 2 and 4ESM). These features have relatively rough shapes and do not appear to be covered by consistent sediment draping, suggesting a relatively young age of formation. Conversely, submarine eruptive centres recognized on the southern flank of Linosa as monogenic, single and composite cones (Figs. 3 and 1ESM) commonly appear with a smoother appearance, indicating sedimentary cover on top. They mostly rise from inter mediate depth (250 570 m), damming the volcaniclastic sediment moving down the submarine flank in small, perched basins (Fig. 4c). These eruptive centres surround the islands' southern part with a semicircular pattern (Figs. 2 and 3), although local NNW SSE to WNW ESE alignments are recognizable in their distribution. Some of them (with summit depth at some hundred m depth) are flat topped cones (Fig. 3 and 1ESM).

In the following sections, eruptive cones observed on the wide submarine portions of Linosa are analyzed from a morphological and morphometric point of view.

4.2. Morphometry of submarine cones

Following the morphometric approach indicated in Section 3.1, we classified the submarine eruptive cones observed in the Linosa offshore on the base of their shape, and measured their main morphological parameters. A total of 41 eruptive centres were mapped and measured: 25 in the northwestern submarine flank, 2 in the western and north eastern flanks, and 14 in the southern sector (Fig. 2 and Table 1ESM). Submarine cones are attributed to five different shape classes (conical/subconical, elliptical/subelliptical, composite, flat topped and star shape, Fig. 7) based on plant and section view and according to Doniz Páez (2015). The conical/subconical shape (Fig. 7a) has a regular form and correspond to 26.8% (11 structures) of the analyzed cones (Fig. 8), while elliptical/subelliptical shape (15 structures, representing 36.6%of the total ones, Figs. 7b and 8) appears to be the result of juxtaposition of circular or sub circular cones along an axial direction, which prob ably indicates a fissural vent. The composite shape (9 structures, 21.9%, Figs. 7c and 8) is also due to the coalescence or grouping of more cones, having both circular and elliptical shape in plant, building up a larger and less regular structure. The flat topped cones are 4 structures (cor responding to 9.8%, Figs. 7d and 8); those located in shallow water (SL1 and SL2 in Figs. 3 1ESM and 2ESM) could be considered as derived by the conical shape, eroded at their top. Finally, a star shape has been recognized in only two eruptive centres (4.9% of the total, Figs. 7d and 8) that are the larger ones observed on the Linosa submarine flanks (Table 1ESM). This peculiar shape likely reflects the relief of radiating intrusion zones (Mitchell, 2001).

Overall, the eruptive centres have heights from 26 m to 265 m with an average value of about 108 ± 54 m (Table 2); this range includes flat topped cones and a few centres affected by summit collapses, their measure having an intrinsic error that is tied to post or *syn* eruptive dynamics. In detail, most (39%) of the eruptive centres have heights from 81 m to 130 m and a significant percentage (32%) has lower heights in the range 40 80 m (ESM1). The average basal diameter of eruptive centres (Wbc in Table 2) is about 617 m ± 241 m. This large associated variability is due to the fact that a reduced number of edi fices have basal diameters lower than 200 m or > 800/1000 m. Actu ally, the 39% of the eruptive centres have basal diameters in the range 400 600 m, and the 27% in the range 600 800 m (Table 1ESM). The basal ratio (bsr), representing the degree of irregularity/ellipsoidity of the centres, varies from 1.03 to 2.45 and its average value is 1.38 ± 0.36 (Table 2). The aspect ratio AR, that defines the relation ship between height and basal diameter, is in the range 0.06 0.30, with an average value of 0.18 ± 0.06 (Table 2). The scatter plot of this parameter shows a linear trend among smaller cones (mostly conical, elliptical and flat topped) and larger cones (mostly composite and star shaped; Fig. 9). Regarding the volume estimated for the cones (total of 2.571 km^3), an average value of 0.063 km^3 ± 0.08 is obtained (Table 2). However, 53.2% of the total volume is made up by 7 largest centres, having a volume > 0,1 km^3 each, located on both the northern and southern flanks (Table 1ESM). The remaining 46.8% is represented by cones ranging in volume between 1×10^3 and 9×10^2 km^3. Fi nally, the maximum slope of the cones ranges between 20° and 40°, with an average value of about 28° ± 4 (Table 2). Table 3 summarizes the main morphological parameters estimated for each typology. It can be noted that star shaped and composite cones are commonly the lar gest ones.

5. Discussion

The study of the wide submarine areas of Linosa, representing the

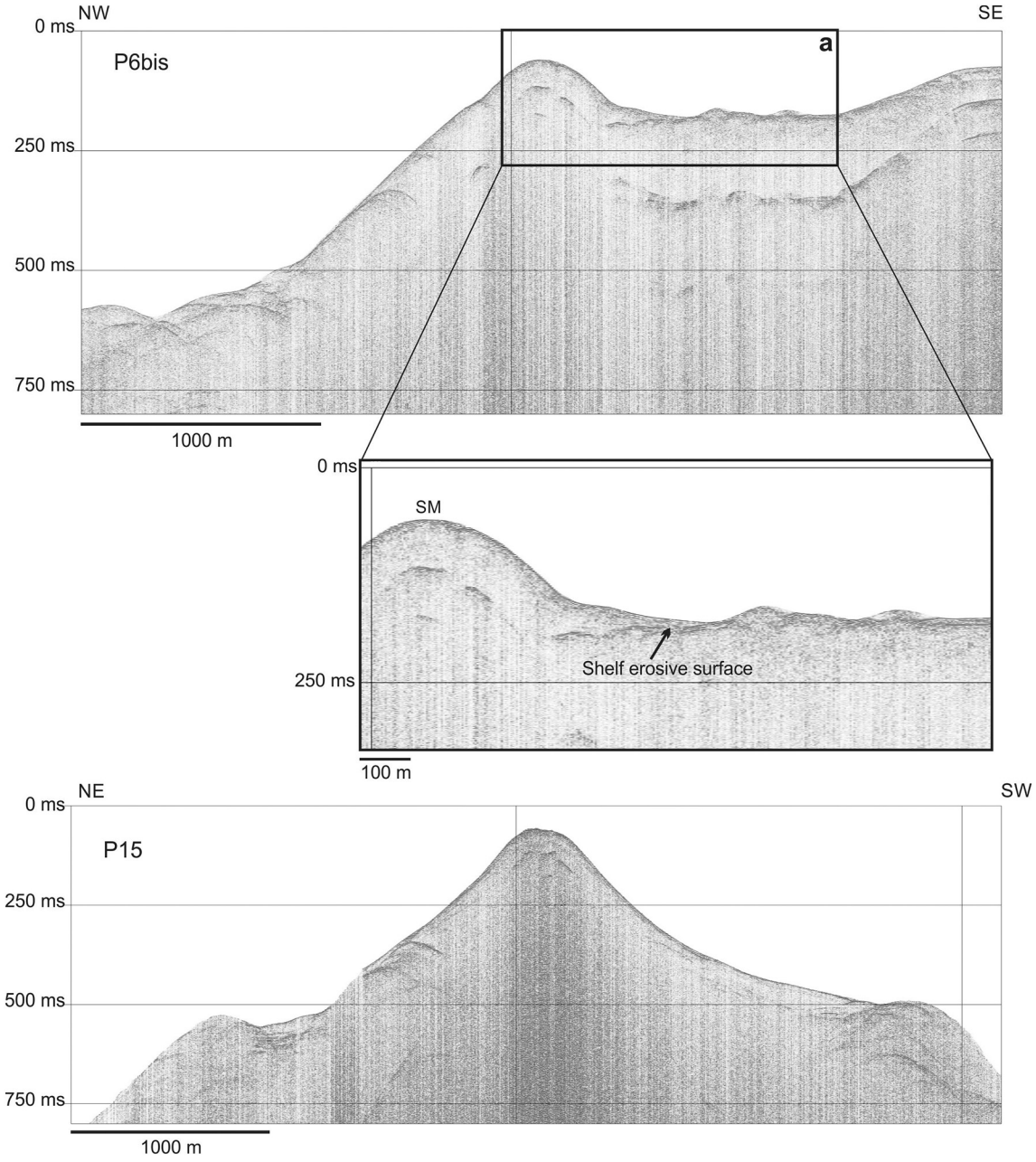

Fig. 6. Sparker profiles P6bis and P15 (location in Fig. 5) across the eruptive cone of Secca Maestra (SM), coalescent with the insular shelf to the northwest of Linosa. The regular shape of the volcanic cone is not affected by erosion and the deposits at its foot overlap the erosive surface of the insular shelf (see zoom a).

~96% of the total extension of the volcanic edifice, allows to enlarge the knowledge of this poorly known volcano and to put new constraints on its development. The submarine setting of Linosa appears to be controlled by the complex interplay between volcanic, tectonic, erosive/depositional processes and Late Quaternary sea level fluctuations. The preferential development of the volcanic edifice for about 20 km in the NW SE direction supports the role of regional tectonics in its evolution, as already suggested by Rossi et al. (1990). This is commonly observed in rift zones, where volcanoes are generally related to extensional processes occurring at the tips of the main strike slip/extensional faults, as a consequence of the local crustal stretching (Ventura et al., 1999 and references herein; Fornaciai et al., 2012). The large number of scoria cones discovered in the submarine portions of Linosa, mostly clustered in linear chains along a NW SE oriented volcanic field, represents another evidence of tectonic control on volcanism, as their morphology and distribution are commonly used as indicator of crustal stress orientation (Connor and Conway, 2000; Tibaldi and Corazzato, 2006; Fornaciai et al., 2012). Submarine volcanic cones rising from the Linosa flanks are analyzed here also from a morphologic and morphometric point of view, showing similarities with those observed in other contexts and at the nearby volcanic edifice of Pantelleria (Calarco, 2011). Finally, starting from its submarine setting we discuss some new evidences on the evolution of the Linosa volcano at its early emersion, based on the occurrence and characteristics of insular shelves in the shallow water portions, and on possible recent most activity, based on the characteristics of eruptive centres on its submarine flanks.

5.1. Submarine eruptive cones

On the submarine flanks of Linosa island we have mapped and identified 41 submarine eruptive cones, rising from depths ranging between ~90 to ~970 m (Tables 2 and 1ESM). Most of the newly

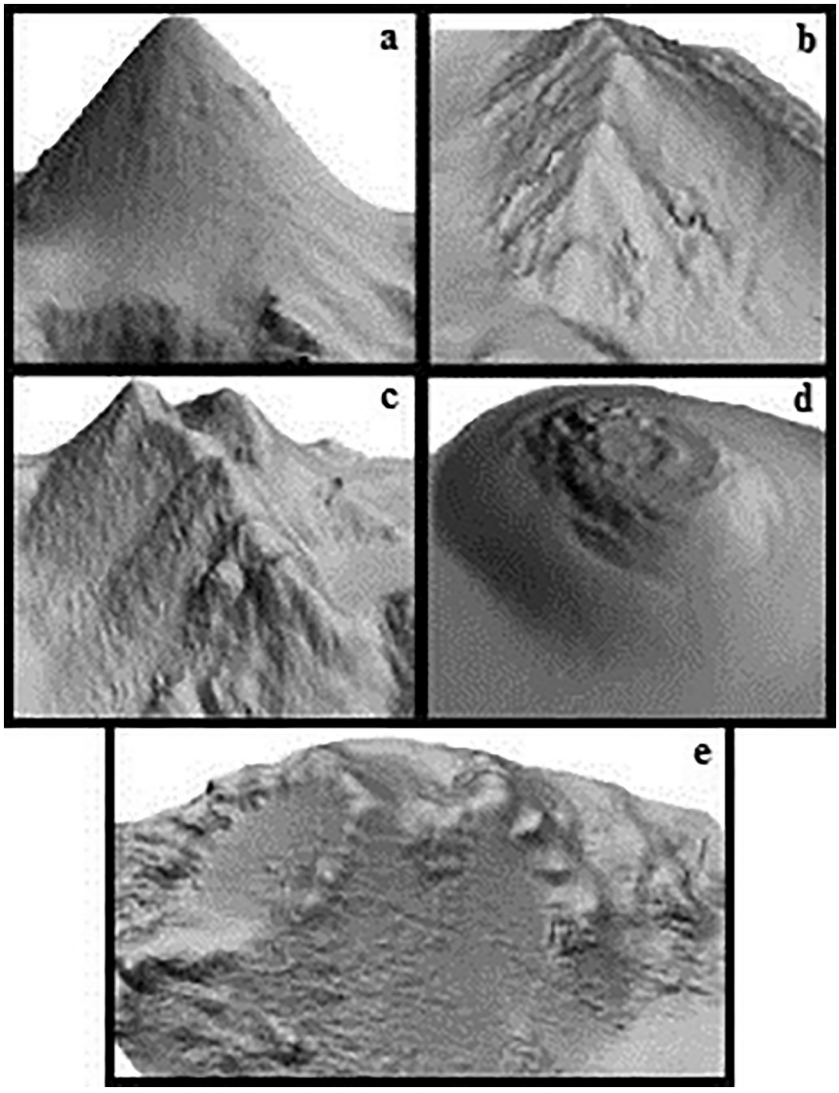

Fig. 7. Main shape typologies of submarine cones recognized at Linosa (a: conical/subconical, b: elliptical/subelliptical, c: composite, d: flat-topped and e: star-shape).

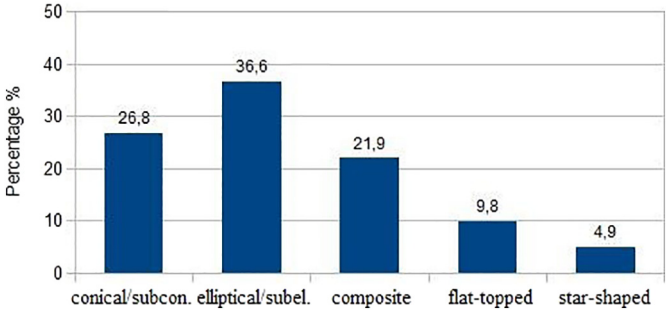

Fig. 8. Statistical distribution of the different typologies of submarine cones.

discovered eruptive vents rise from the northwestern submarine flank of the edifice (up to 10 km far from the island coastline) and consist of single or composite cones with NW SE alignment. The coalescence of a few cones along a magma feeding fissure creates, in fact, elongated or complex structures that are mainly aligned with that trend (Tibaldi and Corazzato, 2006). In the southern portion of Linosa, submarine cones show a semi circular distribution, with local NW SE alignments. The submarine eruptive cones observed at Linosa exhibit a relatively well preserved volcanic morphology that is similar to that of subaerial scoria

Table 2
Average, maximum and minimum values of morphometric parameters estimated for Linosa submarine cones.

Morphometric parameters	Average	Maximum	Minimum
hmax (m)	107.97 ± 54.61	265	26
Zs (m)	364.88 ± 205.77	833	30
Zb (m)	519.24 ± 231.33	968	89
dmax (m)	707.85 ± 286.88	1305	192
dmin (m)	525.73 ± 213.97	980	133
Wbc (m)	616.79 ± 241.20	1143	163
bsr	1.38 ± 0.36	2.45	1.03
Ac (km^2)	0.33 ± 0.28	1	0.02
AR	0.18 ± 0.06	0.30	0.06
Vc (km^3)	0.063 ± 0.08	0.362	0.001
Smax (°)	28.4 ± 4	40	20

cones. This typology is represented by relatively small, commonly monogenetic volcanoes formed by the eruption of low viscosity magma in Strombolian, Hawaiian, sub Plinian to phreatomagmatic eruptions (Sigurdsson et al., 2000; Fornaciai et al., 2012). They commonly occur in groups or fields, some consisting of hundreds of eruptive centres. These volcanoes may be flat topped, cone shaped or horseshoe shaped, but also elongated cones built above fissures with more complex vent

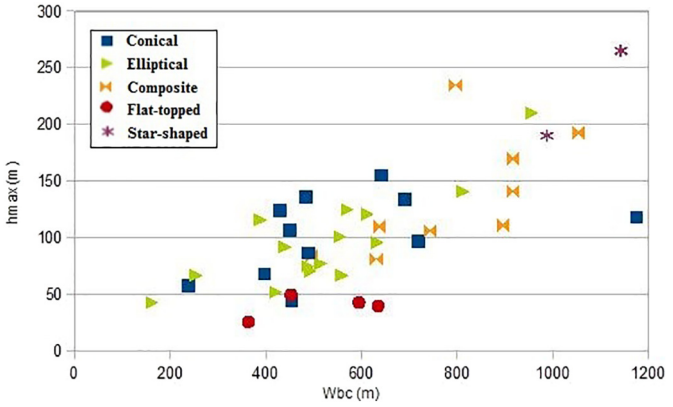

Fig. 9. Scatter plot of aspect ratio (AR), i.e. the relationship between height and basal diameter, for the different shapes recognized in the submarine cones at Linosa.

systems (Sigurdsson et al., 2000).

At Linosa most submarine eruptive cones are small to medium size (Table 3), the star shaped and composite cones being the largest ones, as also observed in oceanic context (Mitchell, 2001). Among morphometric parameters, those indicating the size of the cones (height, area and volume) are more obviously correlated (Romero Ruiz et al., 2000; Calarco, 2011; Doniz Páez, 2015). The scatter plot of aspect ratio (AR, Fig. 9), i.e. the ratio between hmax and the cone width ratio (Wbc), suggests a general increase in height with increasing width, observed also elsewhere (Mitchell et al., 2012). The average value of 0.18 (Table 2) found at Linosa is in agreement with that obtained for many scoria cones worldwide (Favalli et al., 2009 and references herein) and at Pantelleria (0.15; Calarco, 2011) and is a little smaller than AR values of seamounts at Tenerife and in oceanic ridge settings (0.22 0.26, Romero Ruiz et al., 2000 and references herein). The linear trend (Fig. 9) shown by this parameter among smaller cones (mostly conical, elliptical and flat topped) and larger cones (mostly composite and star shaped) is probably due to common eruptive processes and magma physical properties, indicating a self similarity effect observed in other study cases (Calarco, 2011). For instance, they have probably a monogenetic character, as proposed by Rossi et al. (1996) for the vol canic centres on the island that, after their initial activity, do not give evidence of further reactivation.

Conversely, AR values are below 0.11 for flat topped cones (Table 3), as it commonly happens in shallow water (Mitchell, 2001; Mitchell et al., 2012 and references herein). Flat summit volcanic cones may derive from explosive eruptions and through the interaction of magma with ambient water (White et al., 2003) or from continuously overflowing submarine lava ponds (Clague et al., 2000). At Linosa, two flat topped cones located in the SW submarine flank and having summit depth at 192 and 317 m (Table 1ESM) can be related to these processes. Conversely, the truncated shape of the two cones with summit at depth of 30 33 m located on the SE insular shelf (SL1 and SL2 in Figs. 1ESM and 2ESM) suggest the role of wave erosion in recent times or during the last transgression following the Last Glacial Maximum (LGM, see Section 5.2). Studies at Surtla, a parasitic centre of Surtsey (Romagnoli and Jakobsson, 2015) and Graham Bank/Ferdinandea (Coltelli et al., 2016), indicate 55 65 m and 35 40 m as the depth of the present day/recent wave reworking/erosion, respectively (higher at Surtla due to very energetic waves there). Similar to what observed on top of *Secca di Tramontana* (ST in Figs. 5 and 3ESM), the top of Graham Bank Ferdinandea submarine cone is also characterized by low relief, sub concentric ridges/furrows, being likely the result of differential surf erosion of the volcanic substratum. Further examples of similar structures are described for some short lived Surtseyan cones in the Azores islands, such as Princess Alice Bank (Mitchell et al., 2016), and in the shallow water portions of Terceira (Quartau et al., 2014; Casalbore et al., 2015), where these submerged banks have submarine top within 55 m depth.

The occurrence of submarine fields of monogenetic volcanic cones, with comparable size and shape with respect to those mapped at Linosa, has been recently reported by Coltelli et al., (2016), Spatola et al.(2018) and Lodolo et al. (2019) for the southwestern Sicilian offshore. A more punctual morphological comparison is made here with the nearby island of Pantelleria, where morphometric analyses have been carried out on recently identified submarine cones (Calarco, 2011). The morphology and size of the submarine cones found at Pantelleria are similar (slightly larger) to those of Linosa, with heights up to ~350 m and basal widths of ~230 2780 m (Table 4), very similar range of AR values (0.06 0.33) and of bsr values (1.01 2.89, reaching the value of 4 just for one submarine centre; Calarco, 2011). In the NW offshore of Pantelleria, the coalescence of a few cones along an eruptive fissure also creates elongated or complex structures, mostly aligned with the NW SE and WNW ESE trends (Calarco, 2011; Bosman et al., 2011). Only a few flat topped cones are recognized at Pantelleria, with summit depths over −160 m, suggesting that they were not wave eroded. Overall, a similarity between shallower and deeper submarine cones in terms of shape, slope and size has been recognized also at Pantelleria, suggesting that their growth is related to common constructional processes, to a similar monogenetic nature and, probably, basaltic composition (Calarco, 2011).

5.2. Evolution of the Linosa volcanic edifice

The preferential development of the Linosa volcanic edifice in the NW SE direction is also evident from the distribution of insular shelves in its shallow water portions (Figs. 2, 3 and 5). Insular shelves are common features in the submarine flanks of reefless volcanic islands (Quartau et al., 2010; Romagnoli, 2013 and references herein), in dicating those portions of the early emerging volcanic edifices that experienced extensive wave erosion processes down to −100/−130 m during successive cycles of sea level fluctuations, and giving indication on their original extent prior to their erosion. These features have a potential for paleo morphological and relative age reconstructions (Menard, 1983; Llanes et al., 2009; Quartau et al. 2014 and 2015; Romagnoli, 2013; Romagnoli et al., 2018). The distribution and morphology of the insular shelves around Linosa reflect the original extent and paleo morphology of coalescing volcanic centres at the early stage of development of the island, i.e. in the southern and northwestern sectors. In particular, the sub rounded shape of the shelf all around the

Table 3
Main morphometric parameters estimated for the different cones typology.

Typology	Conical/subconical	Elliptical/subelliptical	Composite	Flat-topped	Star-shaped
Heights (m)	43–235	52–141	81–193	26–50[a]	190–225
Widths (m)	163–998	420–813	496–1055	364–650	988–1143
Aspect ratio	0.10–0.30	0.12–0.18	0.13–0.30	0.06–0.11	0.19–0.23
Basal ratio	1.03–1.27	> 1.30	1.07–2.44	1.03–1.30	1.33–1.42
Slope max (°)	20–34	27–32	21–40	21–25	27–30
Volumes (km^3)	0.001–0.2	0.01–0.097	0.022–0.225	0.005–0.028	0.194–0.362

[a] For flat-topped cones, height is underestimated due to post-eruptive erosion.

Table 4
Comparison between minimum and maximum values of morphometric parameters estimated for submarine cones at Linosa and Pantelleria (data from Calarco, 2011).

	Linosa	Pantelleria
No of eruptive cones	41	34
Zs (m)	30/ 833	165/ 614
Zb (m)	89/ 968	328/ 840
hmax (m)	26–265	41–346
Wbc (m)	163–1143	234–2776
bsr	1.03–2.45	1.01–2.89
Ac (km^2)	0.02–1	0.04–6
Vc (km^3)	0.001–0.362	0.001–0.619
AR	0.06–0.30	0.06–0.33
Smax (°)	20–40	21–42

southern part of the island (Fig. 3) is considered to represent the paleomorphology of the volcanic edifice before erosion, indicating that the emerging part of the volcano was originally much larger than conceivable on the basis of its current subaerial extension. The eruptive centre of *Cala Pozzolana di Levante* (CPL in Fig. 3), related to the first eruptive stage recognized on the island ("Paleolinosa" by Lanzafame et al., 1994), is at present almost completely dismantled by the sea apart from scarce outcrops on the SE cliff of the island, and it could partly correspond to the extension of the widely eroded, southern shelf. Similarly, the southwestern shelf could represent the eroded remnants of the *Timpone 1* eruptive centre also related to the "Paleolinosa" eruptive stage (Lanzafame et al., 1994; T1 in Fig. 3). Alternatively, these shelf areas, together with the one to the SE (having no subaerial counterpart), could correspond to the original extension of earlier eruptive centres predating the island emersion and not (or no more) outcropping inland. The shelf observed to the NW of the island shows an elongated morphology, interpreted as derived from the remnants of coalescing, old eruptive centres, presently largely dismantled by marine erosion processes. The sub rounded *Secca di Tramontana* eruptive centre (ST in Fig. 5), with a flattened summit at about 20 m depth, might correspond to the possible shallow water source area for the *Cala Mannarazza* hydroclastic and pyroclastic units outcropping along the northern coast of Linosa (CM in Fig. 5), for which a provenance from the submerged sector has been proposed by Lanzafame et al. (1994) and Rossi et al. (1996).

The age of the earlier volcanic activity is basically unconstrained and almost not determinable, due to the difficulty in sampling the rocky outcrops in the submarine portions, mostly covered by biological encrustations. The polycyclic formation of insular shelves at Linosa, where the volcanic activity on the island is dated from ~1.06 to 0.5 Ma ago (Lanzafame et al., 1994), is consistent with the occurrence of different sea level fluctuations of the late Quaternary that should have affected its submerged flanks (with sea level drops to maximum depth of −127 m in the last 450 ka; Bintanja et al., 2005). The depth of the shelf edge, mostly in the depth range of −100/−130 m, suggests that the volcanic edifice was relatively stable for what regards vertical move ments at least since the LGM (18 20 ka ago). The occurrence of STDs at different depths onto the shelf (Figs. 3 and 5) is likely associated to relative sea level stillstands at the LGM (for the SDT located at the shelf edge, having depositional edge around −100 m, Fig. 4b) and during the following transgression (for the SDT with depositional edge at around −50 m, Fig. 4a). SDTs located at depth similar to the latter one are also observed along other coastal tracts, such as in the Aeolian islands (Chiocci and Romagnoli, 2004; Casalbore et al. 2017 and 2018) and at Pantelleria (Calarco, 2011). The main sources for volcaniclastic de posits that may have fed the thickest STDs at Linosa (located to the south and the west of the island) are represented by the dismantled pyroclastic tuff cones of the *Cala Pozzolana di Levante/Monte Calcarella*, and *Cala Pozzolana di Ponente*, respectively (Fig. 3), widely exposed in the related coastal cliffs (Romagnoli, 2004).

A significant evidence of relatively recent volcanic activity at Linosa is represented by the eruptive centre with very regular conical shape (*Secca Maestra,* SM in Figs. 5 and 3ESM), coalescent with the north western insular shelf and overlapping the shelf erosive surface (Fig. 6a), but not affected by erosion down to −100/120 m as the nearby shelf surface. We believe that this centre, and the deeper, pointy scoria cones rising from the northwestern submarine flank of Linosa with NW SE alignment (Figs. 2 and 4ESM) represent a relatively recent (post 18 ka ago and likely younger) stage of (mostly submarine) eruptive activity of the volcanic edifice, previously unknown. Their relatively uneven morphology and lack of consistent sediment draping, in fact, is different from the setting observed on the southern flank of Linosa, where morphologic and seismo acoustic characteristics of most eruptive centres is consistent with a relatively older age (Figs. 3, 4a and 1ESM). The possible evolution of volcanism proposed for Linosa represents a further similarity with the Pantelleria volcanic edifice, where submarine eruptive cones with well preserved morphologies are identified to the NW of the island, supporting a northwestward propagation of volcanic activity on that side of the volcanic edifice (Calarco, 2011; Bosman et al., 2011).

6. Conclusions

Linosa Island represents only the 4% of a much wider, mostly submarine volcanic edifice that extends for about 20 km in the NW SE direction, evidencing a tectonic control from the main structural system of the Sicily Channel. Until now, the scant knowledge of its submarine extension led to consider this volcanic edifice as extinct. The study of the submarine flanks of Linosa provides new insights on the evolution of this volcanic complex at its early emerging stage and suggests the original extension of related eruptive centres, mostly not (or no more) documented on the island. Conversely, the relatively recent appearance of the several eruptive cones composing the ~10 km long volcanic belt offshore the NW side of the island, supports the occurrence of eruptive activity much younger than the assumed age of volcanism on the island (1.06 0.5 Ma). This has important implications on the potential hazard of this volcanic edifice and on the development of volcanism in the Sicily Channel. Furthermore, the mapping and morphometric study of submarine volcanic cones at Linosa point out a clear similarity with those observed at Pantelleria, also considered associated to a possible northwestward migration of the activity over time (Calarco, 2011).

Declaration of competing interests

The authors declare that they have no known competing financial interests or personal relationships that could have appeared to influence the work reported in this paper.

Supplementary data to this article can be found online at https://doi.org/10.1016/j.margeo.2019.106060.

Acknowledgments

This study benefited from the contribution of the project RITMARE (La Ricerca ITaliana per il MARE http://www.ritmare.it/) Flagship Project, funded by the Italian Ministry of Education, University and Research. We would like to thank the crew of the R/V 'Minerva Uno' for all the support during board and research operations. Patrick Bachèlery, Araceli Munoz Recio and an anonymous reviewer are kindly acknowl edged for their useful suggestions.

References

Babonneau, N., Delacourt, C., Cancouët, R., Sisavath, E., Bachèlery, P., Mazuel, A., Jorry, S.J., Deschamps, A., Ammann, J., Villeneuve, N., 2013. Direct sediment transfer from land to deep-sea: insights into shallow multibeam bathymetry at La Réunion Island. Mar. Geol. 346, 47–57. https://doi.org/10.1016/j.margeo.2013.08.006.

Bintanja, R., Van de Wal, R.S.W., Oerlemans, J., 2005. Modelled atmospheric

temperatures and global sea levels in the past million years. Nature 437, 125–128.
Bosman, A., Chiocci, F., Romagnoli, C., 2009. Morpho-structural setting of Stromboli volcano revealed by high-resolution bathymetry and backscatter data of its submarine portions. Bull. Volcanol. 71 (v9), 1007–1019.
Bosman, A., Calarco, M., Casalbore, D., Conte, A.M., Martorelli, E., Sposato, A., Falese, F., Macelloni, L., Romagnoli, C., Chiocci, F.L., 2011. Volcanic islands: the tip of large submerged volcanoes that only marine geology may reveal (examples from W Pontine Archipelago, Ischia, Stromboli and Pantelleria). In: Brugnoli, E., Cavarretta, G., Mazzola, S., Trincardi, F., Ravaioli, M., Santoleri, R. (Eds.), Marine Research at CNR. (2239-5172) DTA/06-2011. pp. 433–444.
Calanchi, N., Colantoni, P., Rossi, P.L., Saitta, M., Serri, G., 1989. The Strait of Sicily Continental Rift systems: physiography and petrochemistry of the submarine volcanic centers. Mar. Geol. 87, 55–83.
Calarco, M., 2011. Integrated Analyses of the Submarine Volcanic Structures Offshore Pantelleria. PhD. La Sapienza University of Rome.
Casalbore, D., Romagnoli, C., Pimentel, A., Quartau, R., Casas, D., Ercilla, G., Hipolito, A., Sposato, A., Chiocci, F.L., 2015. Volcanic, tectonic and mass-wasting processes offshore Terceira Island (Azores) revealed by high-resolution seafloor mapping. Bull. Volcanol. 77 (v3), 1–19. http://doi:10.1007/s00445-015-0905-3.
Casalbore, D., Falese, F., Martorelli, E., Romagnoli, C., Chiocci, F.L., 2017. Submarine depositional terraces in the Tyrrhenian Sea as a proxy for paleo-sea level reconstruction: Problems and perspective. Quat. Int. 439, 169–180. http://doi:10.1016/j.quaint.2016.02.027.
Casalbore, D., Romagnoli, C., Adami, C., Bosman, A., Falese, F., Ricchi, A., Chiocci, F.L., 2018. Submarine Depositional Terraces at Salina Island (Southern Tyrrhenian Sea) and Implications on the Late-Quaternary Evolution of the Insular Shelf. Geosciences (Switzerland) 8 (v1), 20. https://doi.org/10.3390/geosciences8010020.
Chiocci, F.L., Romagnoli, C., 2004. Terrazzi deposizionali sommersi nelle Isole Eolie. In: Chiocci, F.L., D'Angelo, S., Romagnoli, C. (Eds.), Atlante dei Terrazzi Deposizionali Sommersi Lungo le Coste Italiane. Memorie Descrittive della Carta Geologica d'Italia 58. pp. 81–114.
Civile, D., Lodolo, E., Accettella, D., Geletti, R., Benauraham, Z., Deponte, M., Facchin, L., Ramella, R., Romeo, R., 2010. The Pantelleria graben (Sicily Channel, Central Mediterranean): an example of intraplate “passive” rift. Tectonophysics 490, 173–183.
Clague, D.A., Moore, J.G., Reynolds, J.R., 2000. Formation of submarine flat-topped volcanic cones in Hawaii. Bull. Volcanol. 62, 214–233. https://doi.org/10.1007/s004450000088.
Clague, D.A., Paduan, J.B., Caress, D.W., Moyer, C.L., Glazer, B.T., Yoerger, D.R., 2019. Structure of Lo'ihi Seamount, Hawaii and Lava Flow Morphology From High-Resolution Mapping. Front. Earth Sci. 7 (58). https://doi.org/10.3389/feart.2019.00058. 17pp.
Coastal Consulting Exploration, 2008. Relazione su rilievi marini finalizzati allo studio della morfologia e batimetria dei fondali dell'Isola di Linosa. Internal Technical Report of Marine Protected Area, Lampedusa, Italy.
Colantoni, P., 1975. Note di geologia marina sul Canale di Sicilia. Giorn. Geol. 40, 181–207.
Coltelli, M., Cavallaro, D., D'Anna, G., D'Alessandro, A., Grassa, F., Mangano, G., Patanè, D., Gresta, S., 2016. Exploring the submarine Graham Bank in the Sicily Channel. Ann. Geophys. 59 (2), S0208.
Connor, C.B., Conway, F.M., 2000. Basaltic volcanic field. In: Sigurdsson, H., Houghton, B., McNutt, S., Rymer, H., Stix, J. (Eds.), Encyclopedia of Volcanoes. Encyclopedia of Volcanoes Academic Press, pp. 331–343.
Conte, A.M., Martorelli, E., Calarco, M., Sposato, A., Perinelli, C., Coltelli, M., Chiocci, F.L., 2014. The 1891 submarine eruption offshore Pantelleria Island (Sicily Channel, Italy): Identification of the vent and characterization of products and eruptive style. Geochem. Geophys. Geosyst. 15, 2555–2574.
Di Roberto, A., Bertagnini, A., Pompilio, M., Gamberi, F., Marani, M.P., Rosi, M., 2008. Newly discovered submarine flank eruption at Stromboli volcano (Aeolian islands, Italy). Geophys. Res. Lett. 35, L16310.
Doniz-Páez, J., 2015. Volcanic geomorphological classification of the cinder cones of Tenerife (Canary Islands, Spain). Geomorphology 228, 432–447.
Doniz-Páez, J., Romero Ruiz, C., Coello, E., Guillén, C., Sànchez, N., Garcìa-Cacho, L., Garcìa, A., 2008. Morphological and statistical characterization of recent mafic volcanism on Tenerife (Canary Islands, Spain). J. Volcanol. Geotherm. Res. 173, 185–195.
Favalli, M., Karatson, D., Mazzarini, F., Pareschi, M.T., Boschi, E., 2009. Morphometry of scoria cones located on a volcano flank: a case study from Mt. Etna (Italy) based on high-resolution LiDAR data. J. Volcanol. Geotherm. Res. 186, 320–330.
Fornaciai, A., Favalli, M., Karátson, D., Tarquini, S., Boschi, E., 2012. Morphometry of scoria cones, and their relation to geodynamic setting: a DEM-based analysis. J. Volcanol. Geotherm. Res. 217-218, 56–72.
Grasso, M., Lanzafame, G., Rossi, P.L., Schimncke, H.U., Tranne, C.A., Lajoie, J., Lanti, E., 1991. Volcanic evolution of the island of Linosa Strait of Sicily. Mem. Soc. Geol. It. 47, 509–525.
Innangi, S., Tonielli, R., Romagnoli, C., Budillon, F., Di Martino, G., Innangi, M., Lo Iacono, C., 2018. Seabed mapping in the Pelagie Islands marine protected area (Sicily Channel, southern Mediterranean) using Remote Sensing Object Based Image Analysis (RSOBIA). Mar. Geophys. Res. 1–23. https://doi.org/10.1007/s11001-018-9371-6.
Kerezsturi, A., Nemeth, K., Cronin, S.J., Agustìn-Flores, J., Smith, I.E.M., Lindsay, J., 2013. A model for calculating eruptive volumes for monogenetic volcanoes - implication for the Quaternary Auckland Volcanic Field, New Zealand. J. Volcanol. Geotherm. Res. 266, 16–33.
Lanti, E., Lanzafame, G., Rossi, P.L., Tranne, C.A., Calanchi, N., 1988. Vulcanismo e tettonica nel Canale di Sicilia: l'isola di Linosa. Miner. Petrog. Acta 31, 69–93.
Lanzafame, G., Rossi, P.L., Tranne, C.A., and Lanti, E., 1994. Carta geologica dell'isola di Linosa, scale 1:5.000, Firenze, SELCA.
Llanes, P., Herrera, R., Gomez, M., Munoz, A., Acosta, J., Uchupi, E., 2009. Geological evolution of the volcanic island La Gomera, Canary Islands, from analysis of its geomorphology. Mar. Geol. 264, 123–139.
Lodolo, E., Civile, D., Zecchin, M., Zampa, L.S., Accaino, F., 2019. A series of volcanic edifices discovered a few kilometers off the coast of SW Sicily. Mar. Geol. 416. https://doi.org/10.1016/j.margeo.2019.105999.
Menard, H.W., 1983. Insular erosion, isostasy, and subsidence. Science 220, 913–918.
Mitchell, N.C., 2001. Transition from circular to stellate forms of submarine volcanoes. J. Geophys. Res. 106, 1987–2003.
Mitchell, N.C., Strect, R., Oppenheimer, C., Kay, D., Beier, C., 2012. Cone morphology associated with shallow marine eruptions: east Pico Island, Azores. Bull. Volcanol. 74, 2289–2301.
Mitchell, N.C., Stretch, R., Tempera, F., Ligi, M., 2016. Volcanism in the Azores: a marine geophysical perspective. In: Kueppers, U., Beier, C. (Eds.), Volcanoes of the Azores. Springer-Verlag, Eds, pp. 101–126.
Pope, E.L., Jutzeler, M., Cartigny, M.J.B., Shreeve, J., Talling, P.J., Wright, I.C., Wysoczanski, R.J., 2018. Origin of spectacular fields of submarine sediment waves around volcanic islands. Earth Planet. Sci. Lett. 493, 12–24. https://doi.org/10.1016/j.epsl.2018.04.020.
Quartau, R., Trenhaile, A.S., Mitchell, N.C., Tempera, F., 2010. Development of volcanic insular shelves: insights from observations and modelling of Faial Island in the Azores Archipelago. Mar. Geol. 275, 66–83.
Quartau, R., Hipolito, A., Romagnoli, C., Casalbore, D., Madeira, J., Tempera, F., Roque, C., Chiocci, F.L., 2014. The morphology of insular shelves as a key for understanding the geological evolution of volcanic islands: insights from Terceira Island (Azores). Geochem. Geophys. Geosyst. 15, 1801–1826.
Quartau, R., Madeira, J., Mitchell, N.C., Tempera, F., Silva, P.F., Brandao, F., 2015. The insular shelves of the Faial-Pico Ridge (Azores archipelago): a morphological record of its evolution. Geochem. Geophys. Geosyst. 16, 1401–1420.
Riccò, 1892. Terremoti, sollevamento ed eruzione sottomarina a Pantelleria nella seconda metà dell'ottobre 1891. Boll. Soc. Geogr. Ital. 1–31.
Romagnoli, C., 2004. Terrazzi deposizionali sommersi nell'isola di Linosa (Canale di Sicilia). Mem. Descr. Carta Geol. D'It. 58, 133–140.
Romagnoli, C., 2013. Characteristics and morphological evolution of the Aeolian volcanoes from the study of submarine portions. In: Lucchi, F., Peccerillo, A., Keller, J., Tranne, C.A., Rossi, P.L. (Eds.), The Aeolian Islands Volcanoes. Geological Society, London, Memories 37. pp. 13–26.
Romagnoli, C., Jakobsson, S.P., 2015. Post-eruptive morphological evolution of island volcanoes: Surtsey as a modern case study. Geomorphology 250, 384–396. Romagnoli, C., Casalbore, D., Chiocci, F.L., Bosman, A., 2009a. Offshore evidence of large–scale lateral collapse on the eastern flank of Stromboli, Italy, due to structurally–controlled, bi-lateral flank instability. Mar. Geol. 262, 1–13. https://doi.org/10.1016/j.margeo.2009.02.004.
Romagnoli, C., Kokelaar, P., Casalbore, D., Chiocci, F.L., 2009b. Lateral collapses and active sedimentary processes on the northwestern flank of Stromboli volcano, Italy. Mar. Geol. 265, 101–119. https://doi https://doi.org/10.1016/j.margeo.2009.06.013.
Romagnoli, C., Casalbore, D., et al., 2013. Bathy-morphological setting of the Aeolian Islands, in: Lucchi F., Peccerillo A., Keller J., Tranne C.A. E Rossi P.L. (Eds.), The Aeolian Islands Volcanoes. Geological Society, London, Memoirs, 37, 27–36.
Romagnoli, C., Casalbore, D., Ricchi, A., Lucchi, F., Quartau, R., Bosman, A., Tranne, C.A., Chiocci, F.L., 2018. Morpho-bathymetric and seismo-stratigraphic analysis of the insular shelf of Salina (Aeolian archipelago) to unveil its Late-Quaternary geological evolution. Mar. Geol. 395, 133–151.
Romero Ruiz, C., Garcìa-Cacho, L., Araña, V., Ynnes Luque, A., Felpeto, A., 2000. Submarine volcanism surrounding Tenerife, Canary Islands: implications for tectonic controls, and oceanic shield forming processes. J. Volcanol. Geotherm. Res. 103, 105–119.
Rossi, P.L., Gabbianelli, G., Romagnoli, C., Serri, G., 1990. Ricerche di geologia marina nelle aree vulcaniche del Tirreno meridionale e Canale di Sicilia. Mem. Soc. Geol. It. 45, 927–938.
Rossi, P.L., Tranne, C.A., Calanchi, N., Lanti, E., 1996. Geology, stratigraphy and vulcanological evolution of the island of Linosa (Sicily Channel). Acta Vulcanol. 8, 73–90. Sigurdsson, H., Houghton, B., McNutt, S., Rymer, H., Stix, J., 2000. Encyclopedia of Volcanoes. Academic Press, pp. 361–400.
Somoza, L., González, F.J., Barker, S.J., Madureira, P., Medialdea, T., De Ignacio, C., Palomino, D., 2017. Evolution of submarine eruptive activity during the 2011–2012 El Hierro event as documented by hydroacoustic images and remotely operated vehicle observations. Geochem. Geophys. Geosyst. 18 (v8), 3109–3137. https://doi.org/10.1002/2016GC006733.
Spatola, D., Micallef, A., Sulli, A., Basilone, L., Ferreri, R., Basilone, G., Bonanno, A., Pulizzi, M., Mangano, S., 2018. The Graham Bank (Sicily Channel, central Mediterranean Sea): seafloor signatures of volcanic and tectonic controls. Geomorphology 318, 375–389. https://doi.org/10.1016/j.geomorph.2018.07.006.
Tibaldi, A., Corazzato, C., 2006. Fracture control on type, morphology and distribution of parasitic volcanic cones: an example from Mt. Etna, Italy. J. Volcanol. Geotherm. Res. 158, 177–194.
Tonielli, R., Innangi, S., Di Martino, G., Romagnoli, C., 2019. New bathymetry of the Linosa volcanic complex from multibeamsystems (Sicily Channel, Mediterranean Sea). Journal of Maps 15 (2), 611–618. https://doi:10.1080/17445647.2019.1642807.
Ventura, G., Vilardo, G., Milano, G., Pino, N.A., 1999. Relationships among crustal structure, volcanism and strike-slip tectonics in the Lipari-Vulcano Volcanic Complex (Aeolian Islands, Southern Tyrrhenian Sea, Italy). Phys. Earth Planet. Inter. 116, 31–52.
Watts, A.B., Masson, D.G., 1995. A giant landslide in the north flank of Tenerife, Canary Islands. J. Geophys. Res. 100, 24487–24498.
White, J.D.L., Smellie, J.L., Clague, D.A., 2003. Introduction: A deductive outline and topical overview of subaqueous explosive volcanism. In: White, J.D.L., Smellie, J.L., Clague, D.A. (Eds.), Subaqueous explosive volcanism. 140. American Geophysical Union, Geophysical Monograph, Washington DC, pp. 1–23.